Development of Model Predictive Control for Magnetic Levitation Systems

Lakshmi Dutta
University Science Instrumentation Centre
North Bengal University
Siliguri, West Bengal India 734014
Email: lakshmi@nbu.co.in
Orcid Id: https://orcid.org/0000-0002-4895-8993

***Abstract*—The study of Magnetic Levitation systems(Maglev) has gained significant attention due to their minimal friction and energy-efficient attributes, which are deemed crucial factors. This paper introduces a novel magnetic levitation system implemented through the Simulink environment. The dynamics of Maglev exhibit nonlinearity and high instability, which renders the task of devising a suitable control algorithm even more challenging. The primary objective of this study is to regulate the position of a ferromagnetic ball within the airspace of the nonlinear system. In this investigation, the proposed controller is formulated based on the linear predictive model, derived by approximating the plant's behavior around a known operational point. The efficacy of the proposed control approach is validated through simulation levitation model. The performance of the proposed controller is compared with a existing PID control technique [1] and found better results.**

I. INTRODUCTION

Magnetic levitation systems hold practical significance across diverse engineering applications. Examples include their utilization in high-speed maglev passenger trains, bearings designed for frictionless movement, elevating wind tunnel models, isolating vibrations in delicate machinery, suspending molten metal within induction furnaces, and raising metal slabs during manufacturing processes. Depending on the origin of levitation forces, maglev systems can be categorized as either attractive or repulsive setups. Typically, these types of systems exhibit instability when operated in open-loop configurations and are characterized by complex nonlinear differential equations, which introduce added challenges in controlling them. As a result, a crucial attempt involves the development of high-performance predictive controllers aimed at effectively managing the position of the levitated object.

Recently, numerous studies have emerged in the literature concerning the control of magnetic levitation systems. These conventional practice involved linearizing the magnetic levitation system at the equilibrium point using Taylor-series expansion. Subsequently, controllers like the proportional-integral-derivative (PID) [2] and linear-quadratic regulator (LQR) [3] were designed. However, this linearization approximation method led to reduced robustness in magnetic levitation control systems as certain nonlinear terms were overlooked. The feedback linearization technique has found application in devising control strategies for magnetic levitation systems [4], [5]. This approach aimed to improve upon the drawbacks of the approximation linearization method. The subsequent adoption of the backstepping technique in controller design [6], [7] marked a further step in this direction. In recent years, more advanced control techniques have been proposed to manage levitation in Maglev system. These include adaptive control, robust control, sliding mode control (SMC), or combinations thereof. Authors in [8] introduced an adaptive robust controller for the Maglev transportation system, enhancing robustness against uncertainties, external disturbances. Similarly, [9] put forth a robust controller with a disturbance observer based on an improved suspension force model for Maglev system. [10] employed an adaptive SMC law along with a magnetic flux observer for the magnetic levitation systems, addressing model uncertainty and external disturbances. However, the challenge of chattering remained a significant hurdle in SMC application. Subsequent efforts explored intelligent control methods to tackle the intricate nonlinearity of magnetic levitation systems. [11] introduced a novel fuzzy controller for the levitation system based on the Takagi Sugeno fuzzy model, coupled with a H_∞ robust control law for enhanced robustness against parameter perturbations and external disturbances. Building on this, an improved approach using a parallel-distributed compensation scheme was presented [11], albeit with the challenge of establishing stable fuzzy logic rules. In [12], a fuzzy neural network (NN) was employed to emulate an adaptive observer, forming a control framework for hybrid permanent magnet and electromagnet Maglev transportation systems. This approach exhibited excellent performance due to the model-free nature of NN. However, the methods mentioned earlier have certain limitations when it comes to addressing constraints in the context of magnetic levitation systems. These constraints pertain to real-time requirements that ensure reliability [13], [14]. In the case of Maglev trains, it's essential to consider state constraints such as the air gap, vertical velocity, and acceleration to meet the reliability criteria for aspects like ride comfort, energy efficiency, and system implementation [15]. Model predictive control (MPC) is a widely adopted approach in industrial process control that excels in handling both control and state constraints explicitly and optimally [14]. Model Predictive Control (MPC) encompasses solving an optimal control problem with a finite

horizon that shifts as time progresses [16]. This involves solving the control sequence for the current situation online during each sampling moment, with only the initial control element of the sequence being employed [17]. Additionally, the present state variables of the process are utilized as the starting point for the optimization problem. MPC methods do have a computational cost, which results from the ongoing need for online optimisation, which is one of its limitations. This is a significant barrier for fast-response systems and turns into a major problem for MPC applications. In recent times, researchers have effectively employed MPC across various domains. These include its application in robotics [18], energy-efficient control of twin rotor MIMO system [19], electrical vehicles [20] and power system etc. The MPC approach has also been extended to encompass magnetic levitation ball systems. Authors in [21] proposed a robust MPC for a second-order magnetic levitation ball system, accounting for input and output constraints. In this work, the model uncertainties are also managed using the linear matrix inequalities (LMI) technique. This approach involved a linear approximation model via Taylor-series expansion. Authors in [22] designed a MPC controller for a magnetic levitation ball system grounded in a pre-identified state-dependent model, autoregressive with eXogenous variables (ARX), achieved through a collection of radial basis function neural networks (RBF NNs). Further, in [23], [24] the authors have introduced an explicit model predictive controller (EMPC) for the magnetic levitation system, strategically shifting the optimization process offline to enhance real-time efficiency. They accounted for both input and output constraints for a piece-wise affine (PWA) linear system. Moreover, authors in [25] have introduced a nonlinear MPC (NMPC) approach to the magnetic levitation system. This approach aimed to achieve high control performance by accurately predicting the nonlinear system behavior. Nevertheless, the design complexity associated with NMPC posed computational challenges greater than those of linear MPC schemes, thus restricting the consideration of control constraints to maintain real-time feasibility. The primary aim of this study is to create a linear model predictive control (MPC) approach adapted for a magnetic levitation system with input-output constraints. In this research, prediction models are derived using the physical parameters of the Maglev system as detailed in TABLE I. The suggested control strategy has been assessed through simulations conducted on magnetic levitation systems using three distinct input signals. The simulation outcomes illustrate the tracking capabilities of the proposed control algorithm is better as compared to the existing control technique [1].

II. SYSTEM MODELING

Fig.1 depicts a schematic representation of a Maglev system. The various mechanical parts and its motions can be predicted from this schematic diagram. Magnetic levitation's laboratory setup was created by Feedback Instruments Ltd. and operates in the MATLAB/Simulink environment. The magnetic force balances the gravitational force exerted on the ferromagnetic

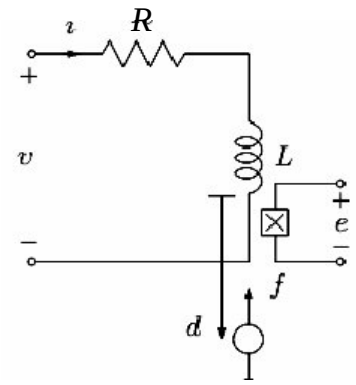

Fig. 1: Schematic diagram of the Maglev system

ball during the operation of the Maglev system. By altering the input current, the magnetic force of the Maglev may be changed. As a result, in the Maglev model, the magnetic force is equal to the square of the electromagnetic coil current. With the aid of the controller, the system receives input from the coil current to regulate the location of the iron ball, which is then balanced in the air space according to the requirement.

TABLE I: Maglev system parameters

Parameter	Value	Unit
β	5.64×10^{-4}	Vm^2
γ	0.31	V/A
α	2.48	V
i_0	1	A
d_0	20	mm
C	2.4×10^{-6}	Kgm^5/s^2
R	2	Ohm
L	15×10^{-3}	H
$m = \frac{M}{4}$	0.02985	Kg

A. STATE SPACE MODEL

The construction of the magnetic levitation system and its parts will be described in this section. The system consists of four electromagnets that act as actuators to apply magnetic forces for accurate position control. Four Hall effect sensors that detect the position of the levitating plate are also included, along with a rigid square plate with four permanent magnets on each corner. The electromagnets are 2 ohm internal-resistance solenoid coils with a 15 mH rating. Linear radiometric Hall Effect sensors with a 50 V/T are used in Hall effects experiments. The neodymium $N52$ disc magnets have a 12.70 mm diameter and a 6.35 mm thickness, and they are used as permanent magnets. The electromagnetic levitation system model is shown in Fig. 2, where R denotes the coil's resistance, L denotes its inductance, v denotes the voltage across the electromagnet, i denotes the current flowing through it, m denotes the mass of the levitating system, g denotes the acceleration caused by gravity, d denotes the vertical position of the ball measured from the bottom, f denotes the force on the levitating system generated by the electromagnet and

e denotes the voltage across the Hall effect sensor. The force generated by the electromagnet is formulated as:

$$F_{mag} = C\frac{i(t)}{d^3} \tag{1}$$

where d is the vertical position and C is a turn constant. From (1) we got

$$M\ddot{d} = mg - C\frac{i(t)}{d^3} \tag{2}$$

where m is the mass of the levitating magnet and g is the gravity of acceleration. The power supply and electromagnetic coil can be related electrically by using the following expression:

$$v(t) = R.i(t) + L\frac{di}{dt} \tag{3}$$

where R and L are resistance and inductance of the electromagnet respectively. Now consider the following perturbations with respect to the change of them

$$i(t) = i_0 + \Delta i(t) \tag{4}$$

$$d(t) = d_0 + \Delta d(t) \tag{5}$$

$$v(t) = v_0 + \Delta v(t) \tag{6}$$

where the voltage needed to suspend the levitating plate at d_o is called v_o. Under this perturbation, it is possible to linearize the dynamics (2) and (3) around an operational point $(i_0; d_0; v_0)$ as

$$m\ddot{\Delta}d = \left(\frac{3Ci_0}{d_0^4}\right)\Delta d - \left(\frac{C}{d_0^3}\right)\Delta i \tag{7}$$

$$\dot{\Delta}i = \left(\frac{R}{L}\right)\Delta i - \left(\frac{1}{L}\right)\Delta v \tag{8}$$

where $\Delta i, \Delta v, \Delta d$ represents the linearization of the system around its equilibrium point. The transfer function from Δv to Δd is obtained by removing Δi in equation (8) and using Laplace transforms as

$$\frac{\Delta D(s)}{\Delta V(s)} = \frac{-\frac{g^R}{v_0}}{(Ls+R)(s^2 - \frac{3Ci_0}{md_0^4})} \tag{9}$$

where $\Delta V(s)$ and $\Delta D(s)$ denote the Laplace transforms of $\Delta v(t)$ and $\Delta d(t)$, respectively. The output voltage of the Hall sensor is as follows.

$$e(t) = \alpha + \frac{\beta}{d^2} + \gamma i(t) \tag{10}$$

where α, β, γ are constant sensor parameters. A linearization of (10) around $e(t) = e_0 + \Delta e$ results in

$$e(t) = \frac{2\beta}{d^3}\Delta d + \gamma\Delta i \tag{11}$$

where Δe is the sensor voltage. We find the following relationship between the electromagnet voltage $\Delta V(s)$ and a sensor voltage perturbation $\Delta E(s)$ by applying Laplace transform to (11) and utilising $I(s) = \Delta V(s)/(L_s + R)$ from (3) and the representation in (9) as follows:

$$\frac{\Delta E(s)}{\Delta V(s)} = \frac{\gamma(s^2 - \frac{3Ci_0}{md_0^4}) + (\frac{2\beta RC}{md_0^6})}{(Ls+R)(s^2 - \frac{3Ci_0}{md_0^4})} \tag{12}$$

Once the second derivative of (7) and the first derivative of (8) have been applied, equation (12) can also be represented in state space form. As a result, the linearized model of Equation (12) can be represented in state space as follows:

$$\begin{bmatrix}\dot{x}_1\\ \dot{x}_2\\ \dot{x}_3\end{bmatrix} = \begin{bmatrix}0 & 1 & 0\\ 3\frac{C}{m}\frac{i_0}{d_0^4} & 0 & -\frac{C}{m}\frac{1}{d_0^3}\\ 0 & 0 & -\frac{R}{L}\end{bmatrix}\begin{bmatrix}x_1\\ x_2\\ x_3\end{bmatrix} + \begin{bmatrix}0\\ 0\\ \frac{1}{L}\end{bmatrix}u \tag{13}$$

The measured output system (y) can be obtained after simplified Equation (11),where $(\Delta e = y, \Delta d = x_1, and \Delta i = x_3)$

$$y = \begin{bmatrix}-2\frac{\beta}{d^3} & 0 & \gamma\end{bmatrix}\begin{bmatrix}x_1\\ x_2\\ x_3\end{bmatrix} \tag{14}$$

Suppose that $x = [x1x2x3] = [d\dot{d}i]$ is the state of the system, where d is the controlled output, $y = e$ is the measured output and $u = v$ is the control input. By substituting system parameters in TABLE I into (12) we get

$$G(s)H(s) = \frac{20.66s^2 + 61803}{s^3 + 132.5s^2 - 1471s - 194900} \tag{15}$$

The numerical values of the state space equations are given below

$$\begin{bmatrix}\dot{x}_1\\ \dot{x}_2\\ \dot{x}_3\end{bmatrix} = \begin{bmatrix}0 & 1 & 0\\ 1471 & 0 & -9.81\\ 0 & 0 & -133\end{bmatrix}\begin{bmatrix}x_1\\ x_2\\ x_3\end{bmatrix} + \begin{bmatrix}0\\ 0\\ 66.66\end{bmatrix}u \tag{16}$$

$$y = \begin{bmatrix}-144 & 0 & 0.31\end{bmatrix}\begin{bmatrix}x_1\\ x_2\\ x_3\end{bmatrix} \tag{17}$$

III. Control Design

A. PID control design

This section aims to illustrate the fundamental structure of a PID controller in the context of closed-loop control for the magnetic levitation system, with the objective of maintaining the ball's position at the desired level. In order to explain the PID controller for a levitation system, it's necessary to possess an appropriate mathematical model of the magnetic levitation system. It can be accomplished through the linearization of all of the elements of the magnetic levitation system. The transfer functions of the aforementioned components, coupled with the PID controller, are presented in Fig.2. Essentially, the controlled magnetic levitation system operates based on error detection. The difference between the reference position and actual position is known as positional error $e(t)$. Subsequently, the PID controller intervenes to regulate this error, enhancing the dynamic response and mitigating steady-state error. The general form of this PID controller is expressed as follows [18]:

$$u(t) = K_p\left(e(t) + \frac{1}{T_i}\int_0^t e(\tau)d\tau\right) + T_d\frac{\partial e(t)}{\partial t} \tag{18}$$

where $u(t)$ denote the control signal K_p the proportional gain, T_i integral time T_d derivative time, and $e(t)$ the difference between the reference point and actual plant.

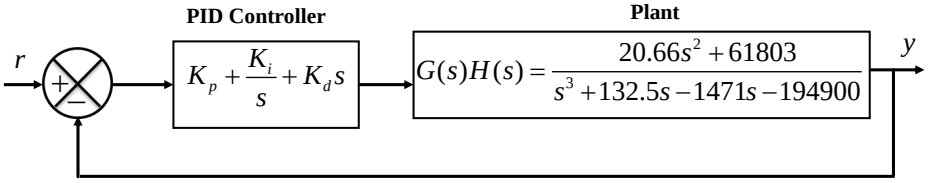

Fig. 2: Magnetic levitation system with the PID controller

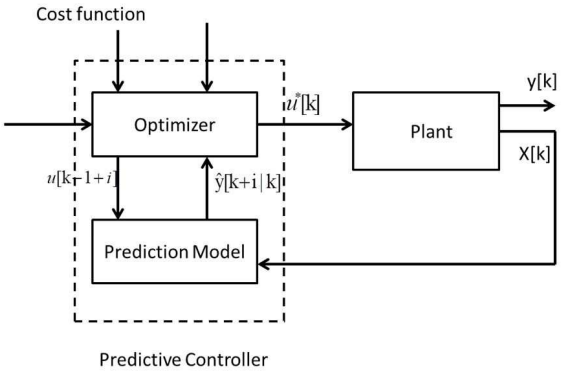

Fig. 3: Block diagram for model predictive controller

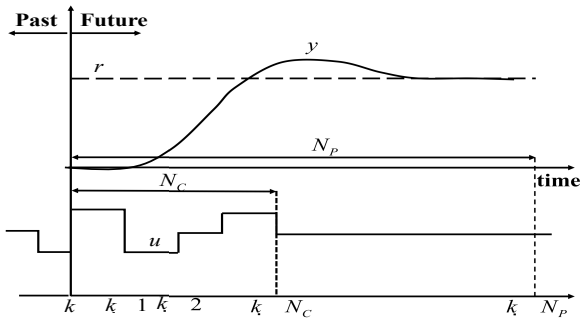

Fig. 4: Basic MPC concept

B. Model predictive control design

This article describes how to create a linear MPC to increase the precision of a Maglev system's control design. Fig.3 depicts the fundamental block diagram of the MPC. Following is a representation of the discrete-time linear state-space model of the Maglev system:

$$\begin{aligned} x(k+1) &= \mathcal{A}_p x(k) + \mathcal{B}_p u_p(k), \\ y(k) &= \mathcal{C}_p x(k) + \mathcal{D}_p u_p(k), \end{aligned} \tag{19}$$

where $x\,(k)$ is a representation of the state vector at instant k^{th}. Similar to this, at the k^{th} instant, $y\,(k)$ and $u_p\,(k)$ represent the system output and control input, respectively. A model predictive controller has a built-in model that predict the future behavior of the plant over a given prediction horizon, or N_p. The optimal control problem is online solved in MPC to identify the control input. The predicted output depends on the assumed input trajectory $u_p\,(k+j\,|k)$ for $j = 0, 1, ..., N_p - 1$. The fundamental concept is to choose that input which gives the best-predicted behavior [**?**].Fig.4 shows the basic concept of linear MPC, where N_p is the prediction horizon and N_c is the control horizon. At each sample instant k, the MPC predict the future outputs at a predetermined horizon, N_p. The predicted output $y\,(k+j\,|k)$, for $j = 0, 1, ..., N_p - 1$, not only depend on the previous outputs and control inputs of the system but also it depends on the future control signal $u_p\,(k+j\,|k)$ for $j = 0, 1, ..., N_p - 1$. To solve the optimization problem of MPC, the interrelation between the inner model output and input of the system needs to be determined. If the input-output relationship is linear during the predefined interval, then the optimization problem can be solved by a linear-quadratic problem. The model state variable within the prediction horizon interval can be determined as:

$$\begin{aligned} \hat{x}\,(k+2\,|k\,) &= \mathcal{A}_p\,(k+1\,|k\,)\,\hat{x}\,(k+1\,|k\,) \\ &\quad + \mathcal{B}_p\,(k+1\,|k\,)\,\hat{u_p}\,(k+1\,|k\,). \end{aligned} \tag{20}$$

(20) can be represented as:

$$\begin{aligned} \hat{x}\,(k+2\,|k\,) &= \mathcal{A}_p\,(k+1\,|k\,)\,\mathcal{A}_p\,(k\,|k\,)\,x\,(k) \\ &\quad + \mathcal{A}_p\,(k+1\,|k\,)\,\mathcal{B}_p\,(k\,|k\,)\,\hat{u_p}\,(k\,|k\,) \\ &\quad + \mathcal{B}_p\,(k+1\,|k\,)\,\hat{u_p}\,(k+1\,|k\,), \\ &\vdots \\ \hat{x}\,(k+N_p\,|k\,) &= \mathcal{A}_p\,(k+N_p-1\,|k\,)\,\hat{x}\,(k+N_p-1\,|k\,) \\ &\quad + \mathcal{B}_p\,(k+N_p-1\,|k\,)\,\hat{u_p}\,(k+N_p-1\,|k\,). \end{aligned} \tag{21}$$

The control inputs are changed during the control horizon interval and after that it will remain constant.

$$\begin{aligned} \hat{u_p}\,(k+j\,|k\,) &= \hat{u_p}\,(k+N_c-1\,|k\,), \\ & N_c \le j \le N_p - 1. \end{aligned} \tag{22}$$

The relation between inputs and the change of inputs are as follows.

$$\hat{u_p}\,(k+j\,|k\,) = u_p\,(k-1) + \sum_{j=0}^{N_c-1} \Delta\hat{u_{p_i}}\,(k+j\,|k\,) \tag{23}$$
$$j = 0, 1, ..., N_c - 1.$$

Substituting (23) into (22) the state variable model can be represented as:

$$\begin{aligned} X(k) &= \mathcal{Z}_{\mathcal{A}_p}(k)\,x(k) + \mathcal{Z}_{\mathcal{B}_p}(k)\,u_p(k-1) \\ &\quad + \mathcal{Z}_{U_p}(k)\,\Delta U_p(k), \end{aligned} \tag{24}$$

where $X(k) = \begin{bmatrix} \hat{x}(k+1\,|k) \\ \hat{x}(k+2\,|k) \\ \vdots \\ \hat{x}(k+N_p\,|k) \end{bmatrix}$; $\mathcal{Z}_{\mathcal{B}_p}(k) = \begin{bmatrix} \mathcal{Z}_{1,1}(k) \\ \mathcal{Z}_{2,1}(k) \\ \vdots \\ \mathcal{Z}_{N_p,1}(k) \end{bmatrix}$;

$$\mathcal{Z}_{\mathcal{A}_p}(k) = \begin{bmatrix} \mathcal{A}_p(k\,|k) \\ \mathcal{A}_p(k+1\,|k\,|k)\,\mathcal{A}_p(k\,|k) \\ \vdots \\ \prod_{j=1}^{N_p} \mathcal{A}_p(k+N_p-j\,|k) \end{bmatrix},$$

$$S_{U_p}(k) = \begin{bmatrix} \mathcal{Z}_{1,1}(k) & 0 & \cdots & 0 \\ \mathcal{Z}_{2,1}(k) & \mathcal{Z}_{2,2}(k) & \cdots & 0 \\ \vdots & \vdots & \ddots & \vdots \\ \mathcal{Z}_{N_p,1}(k) & \mathcal{Z}_{N_p,1}(k) & \cdots & \mathcal{Z}_{N_p,N_p}(k) \end{bmatrix}; \text{ and}$$

$$\Delta U_p(k) = \begin{bmatrix} \Delta\hat{u_p}(k\,|k) \\ \Delta\hat{u_p}(k+1\,|k) \\ \vdots \\ \Delta\hat{u_p}(k+N_c-1\,|k) \end{bmatrix}.$$

Each elements of $\mathcal{Z}_{\mathcal{A}_p}(k)$ and $\mathcal{Z}_{\mathcal{B}_p}(k)$ are given as:

$\mathcal{Z}_{1,1}(k) = \mathcal{B}_p(k\,|k)$,

$\mathcal{Z}_{2,1}(k) = \mathcal{A}_p(k+1\,|k)\,\mathcal{B}_p(k\,|k) + \mathcal{B}_p(k+1\,|k)$,

$\mathcal{Z}_{2,2}(k) = \mathcal{B}_p(k+1\,|k)$,

$\mathcal{Z}_{N_p,1}(k) = \sum_{l=0}^{N_p-2}\left(\prod_{j=1}^{N_c-1-l} \mathcal{A}_c(k+N_p-j\,|k)\right)$
$\mathcal{B}_p(k+l\,|k) + \mathcal{B}_p(k+N_p-1\,|k)$,

$\mathcal{Z}_{N_p,N_c}(k) = \sum_{l=N_c-1}^{N_p-2}\left(\prod_{j=1}^{N_p-1-l} \mathcal{A}_p(k+N_p-j\,|k)\right)$
$\mathcal{B}_p(k+l\,|k) + \mathcal{B}_p(k+N_p-1\,|k)$.

The predicted output of the system can be defined as:

$$Y(k) = \mathcal{Z}_{\mathcal{C}_p} X(k), \tag{25}$$

where

$$Y(k) = \begin{bmatrix} \hat{y}(k+1\,|k) \\ \hat{y}(k+2\,|k) \\ \vdots \\ \hat{y}(k+N_p\,|k) \end{bmatrix};$$

$$\mathcal{Z}_{\mathcal{C}_p}(k) = \begin{bmatrix} \mathcal{C}_p(k+1\,|k) & \cdots & 0 \\ 0 & \cdots & \vdots \\ \vdots & \ddots & \vdots \\ 0 & \cdots & \mathcal{C}_p(k+N_p\,|k) \end{bmatrix}.$$

Furthermore, by substituting (24) into (25), the output equation rearranged as follows.

$$\begin{aligned} Y(k) &= \mathcal{Z}_{\mathcal{C}_p}(k)\,\mathcal{Z}_{\mathcal{A}_p}(k)\,x(k) + \mathcal{Z}_{\mathcal{C}_p}(k)\,\mathcal{Z}_{\mathcal{B}_p}(k)\,u_p(k-1) \\ &\quad + \mathcal{Z}_{\mathcal{C}_p}(k)\,\mathcal{Z}_{U_p}(k)\,\Delta u_p(k). \end{aligned} \tag{26}$$

C. Objective function and constrains:

By minimising the objective/cost function specified along the prediction horizon N_p, it is possible to determine the ideal input to the magnetic levitation system. The objective function is described as the total future error between the desired input and predicted output along the prediction horizon N_p and the total future error between the predicted control inputs along the control horizon N_c. Therefore, the cost function can be defined as follows

$$\begin{aligned} J(k) &= \sum_{j=1}^{N_p} e(k+j)^T \delta(j)\, e(k+j) \\ &\quad + \sum_{j=1}^{N_c} [\Delta\hat{u_p}(k+j-1)]^T \lambda(j)\, [\Delta\hat{u_p}(k+j-1)], \end{aligned} \tag{27}$$

where $e(k+j) = [r(k+j) - \hat{y}(k+j\,|k)]$. The constrains on the control inputs, outputs and the input increments are represented as:

$$y_{\min} \le \hat{y}(k+j\,|k) \le y_{\max}, \qquad j = 1, 2, ..., N_{p,},$$

$$u_{p_{\min}} \le \hat{u_p}(k+j-1\,|k) \le u_{p_{\max}}, \qquad j = 1, 2, ..., N_{c,},$$

$$\Delta u_{p_{\min}} \le \Delta\hat{u_p}(k+j-1\,|k) \le \Delta u_{p_{\max}}, j = 1, 2, ..., N_{c,},$$

where r is the future inputs of the system, $\delta(j)$ is the positive definite error weighting matrix, $\lambda(j)$ is the positive semi-definite control weighting matrix. Further the cost function can be written as:

$$J(k) = E(k)^T Q E(k) + \Delta U_p{}^T(k)\, R \Delta U_p(k), \tag{28}$$

where

$$E(k) = [\mathcal{Z}_r(k) - Y(k)];\ \mathcal{Z}_r(k) = \begin{bmatrix} r(k+1) \\ r(k+2) \\ \vdots \\ r(k+N_p) \end{bmatrix};$$

$$Q = \begin{bmatrix} \delta(1) & 0 & \cdots & 0 \\ 0 & \delta(1) & \cdots & 0 \\ \vdots & \vdots & \ddots & \vdots \\ 0 & 0 & \cdots & \delta(N_p) \end{bmatrix};$$

$$R = \begin{bmatrix} \lambda(1) & 0 & \cdots & 0 \\ 0 & \lambda(1) & \cdots & 0 \\ \vdots & \vdots & \ddots & \vdots \\ 0 & 0 & \cdots & \lambda(N_c) \end{bmatrix}.$$

The linear quadratic function can be obtained by substituting the equation (26) into (28) as follows.

$$\begin{aligned} J(k) &= \frac{1}{2}\Delta U_p{}^T(k)\, H(k)\, \Delta U_p(k) \\ &\quad + \Delta U_p{}^T(k)\, G(k) + c(k), \end{aligned} \tag{29}$$

TABLE II: Controller parameters

Controller	Parameter	Value
MPC	N_p	20
	N_c	10
	$\delta(j)$	$\begin{bmatrix} 1 & 0 \\ 0 & 5 \end{bmatrix}$
	$\lambda(j)$	$0.002I_{2\times 2}$
	T_s	$0.01s$
	u_min	$-2.5v$
	u_max	$2.5v$
PID	K_p	10
	K_i	4
	K_d	0.2

where

$$\begin{aligned} H(k) &= 2\left(\mathcal{Z}_{U_p}^T(k)\,\mathcal{Z}_{C_p}^T(k)\,Q\mathcal{Z}_{C_p}(k)\,\mathcal{Z}_{U_p}(k)+R\right), \\ G(k) &= -2\mathcal{Z}_{U_p}^T(k)\,\mathcal{Z}_{C_p}^T(k)\,QE(k), \\ c(k) &= E^T(k)\,QE(k), \\ E(k) &= \mathcal{Z}_r(k)-\mathcal{Z}_{C_p}(k)\,\mathcal{Z}_{\mathcal{A}_p}(k)\,x(k) \\ &\quad -\mathcal{Z}_{C_p}(k)\,\mathcal{Z}_{\mathcal{B}_p}(k)\,u_p(k-1). \end{aligned}$$

To ensure the stability of the control method at each sampling period, the optimisation problem for the proposed adaptive MPC and extra input and output constraints are implemented.

IV. Simulation Results and Discussion:

In this study, the linearized representation of the magnetic levitation system has been developed using the MATLAB Simulink platform, with parameters set to their nominal values as outlined in TABLE I. The initial state variable value for the system has been established as zero. The controller parameters for both the proposed MPC algorithm and the PID controller can be found in TABLE II. The performance of the controller are evaluated in simulation by applying two different reference signals.

1) Case1: In this case, a desired step input signal with amplitude $0.3mm$ is applied to the Maglev model. In Fig.5, a simulated comparison between the proposed MPC and the existing PID controller [1] for step signal tracking is shown. The control inputs produced by the proposed and existing PID controller are also displayed in Fig.6. These data show that, in comparison to other control algorithms already in use, the proposed MPC exhibits better regulation response, rapid convergence, and very minimal steady-state error [1].

2) Case2: In Fig.7, the Maglev response for a square wave reference with an amplitude of $0.3mm$ and the period of $50s$ is shown. In this instance, the square wave is used to verify the controller's performance in the event of abrupt changes in the direction of the input signal. As shown in Fig.8, the resulting performance of the MPC is improved compared to the existing PID controller [1].

Table III tabulates the comparative tracking results of the proposed MPC with the existing controllers developed in [1]. As can be observed from Table III, the proposed MPC

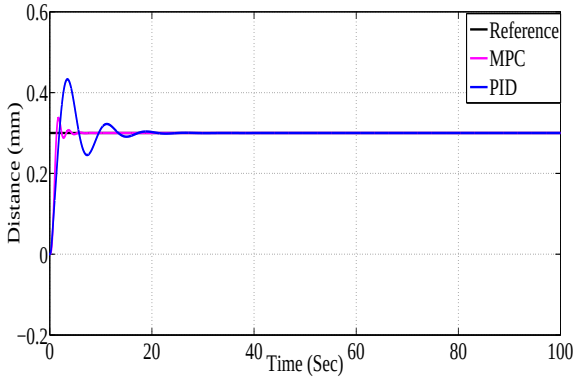

Fig. 5: Step response for magnetic levitation system in simulation

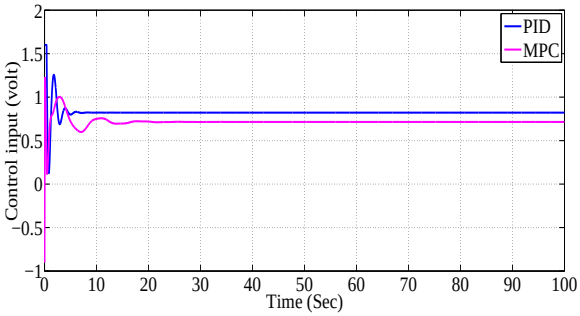

Fig. 6: Control input for step signal in simulation

gives 44.70%, 62.25% and 65.92% lower RMSE, ISE and IAE values as compared to PID [1] control algorithm for case 1. While for case2, it gives 4.04%, 7.88% and 51.02% lower RMSE, ISE and IAE values as compared to PID [1] respectively. Furthermore, Table III shows that the suggested MPC is more energy-efficient than the controllers developed in [1]. The proposed MPC provides 11.2% lower $\|u\|_2$ value for case 1 and 35.76%, lower $\|u\|_2$ value for case 2 of PID [1] controller, respectively.

TABLE III: Performance analysis for both the Case 1 and Case 2

Control Action		Performance Specification					
		M_p	RMSE	ISE	IAE	TV	$\|u\|_2$
Case 1	MPC	12.49	0.094	62.07	209.8	3.49	201.9
	PID [1]	44.4	0.170	168.9	855.1	4.7	227.4
Case 2	MPC	24.66	0.095	906.7	$2.4e^{03}$	30.8	323.8
	PID [1]	69.7	0.09	984.3	$4.9e^{03}$	402.5	504.05

V. Conclusion

The article introduces a linear model predictive control (MPC) algorithm designed for an electromagnetic ball suspension system that is characterized by substantial nonlinearity. To ensure a balanced evaluation, an existing PID control algorithm having the same parameter as [1] has also been

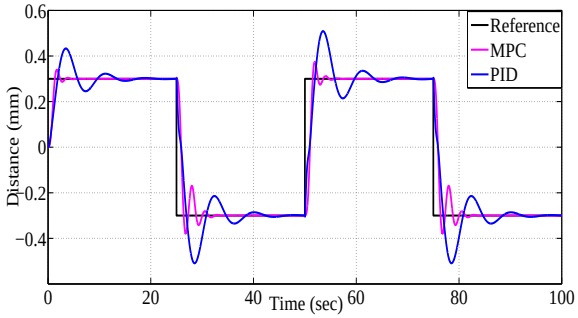

Fig. 7: Square response for magnetic levitation system in simulation

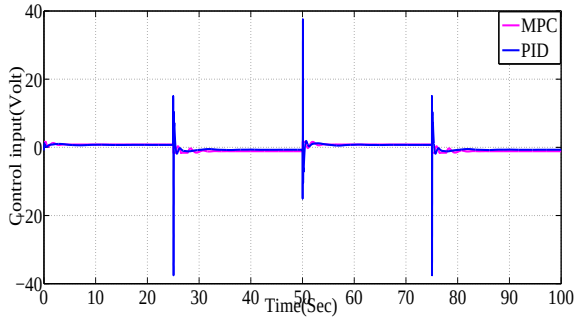

Fig. 8: Control input for square signal in simulation

implemented. The effectiveness of the proposed control algorithm has been successfully demonstrated through validation within a simulation environment, using three distinct reference signals. The resulting output confirms that the proposed controller significantly enhances efficiency in achieving desired trajectory tracking, when compared with the performance of the existing control algorithm [1].

REFERENCES

[1] M. H. Yaseen and H. J. Abd, "Modeling and control for a magnetic levitation system based on simlab platform in real time," *Results in Physics*, vol. 8, pp. 153–159, 2018.

[2] S. Yadav, S. Verma, and S. Nagar, "Optimized pid controller for magnetic levitation system," *Ifac-PapersOnLine*, vol. 49, no. 1, pp. 778–782, 2016.

[3] A. Winursito and G. Pratama, "Lqr state feedback controller with precompensator for magnetic levitation system," in *Journal of Physics: Conference Series*, vol. 2111, no. 1. IOP Publishing, 2021, p. 012004.

[4] S. K. Pradhan and B. Subudhi, "Nonlinear control of a magnetic levitation system using a new input-output feedback linearization," *IFAC-PapersOnLine*, vol. 49, no. 1, pp. 332–336, 2016.

[5] Z.-J. Yang and M. Minashima, "Robust nonlinear control of a feedback linearizable voltage-controlled magnetic levitation system," *IEEJ Transactions on Electronics, Information and Systems*, vol. 121, no. 7, pp. 1203–1211, 2001.

[6] A. S. Malik, I. Ahmad, A. U. Rahman, and Y. Islam, "Integral backstepping and synergetic control of magnetic levitation system," *IEEE Access*, vol. 7, pp. 173 230–173 239, 2019.

[7] Z.-J. Yang, K. Kunitoshi, S. Kanae, and K. Wada, "Adaptive robust output-feedback control of a magnetic levitation system by k-filter approach," *IEEE Transactions on Industrial Electronics*, vol. 55, no. 1, pp. 390–399, 2008.

[8] R. H. Milani, H. Zarabadipour, and R. Shahnazi, "An adaptive robust controller for time delay maglev transportation systems," *Communications in Nonlinear Science and Numerical Simulation*, vol. 17, no. 12, pp. 4792–4801, 2012.

[9] H.-S. Lee, J. Back, and C.-S. Kim, "Disturbance observer-based robust controller for a multiple-electromagnets actuator," *IEEE Transactions on Industrial Electronics*, 2023.

[10] J. Xu, Y. Sun, D. Gao, W. Ma, S. Luo, and Q. Qian, "Dynamic modeling and adaptive sliding mode control for a maglev train system based on a magnetic flux observer," *Ieee Access*, vol. 6, pp. 31 571–31 579, 2018.

[11] Y.-G. Sun, J.-Q. Xu, C. Chen, and G.-B. Lin, "Fuzzy h infinity robust control for magnetic levitation system of maglev vehicles based on ts fuzzy model: Design and experiments," *Journal of Intelligent & Fuzzy Systems*, vol. 36, no. 2, pp. 911–922, 2019.

[12] R.-J. Wai, M.-W. Chen, and J.-X. Yao, "Observer-based adaptive fuzzy-neural-network control for hybrid maglev transportation system," *Neurocomputing*, vol. 175, pp. 10–24, 2016.

[13] J. Mao and C. G. Cassandras, "Optimal control of multilayer discrete event systems with real-time constraint guarantees," *IEEE Transactions on Systems, Man, and Cybernetics: Systems*, vol. 44, no. 10, pp. 1425–1434, 2014.

[14] L. Dutta and D. Kumar Das, "Adaptive model predictive control design using multiple model second level adaptation for parameter estimation of two-degree freedom of helicopter model," *International Journal of Robust and Nonlinear Control*, vol. 31, no. 8, pp. 3248–3278, 2021.

[15] W. Hu, Y. Zhou, Z. Zhang, and H. Fujita, "Model predictive control for hybrid levitation systems of maglev trains with state constraints," *IEEE Transactions on Vehicular Technology*, vol. 70, no. 10, pp. 9972–9985, 2021.

[16] L. Dutta and D. K. Das, "Nonlinear disturbance observer-based adaptive nonlinear model predictive control design for a class of nonlinear mimo system," *International Journal of Systems Science*, vol. 53, no. 9, pp. 2010–2031, 2022.

[17] D. Q. Mayne, J. B. Rawlings, C. V. Rao, and P. O. Scokaert, "Constrained model predictive control: Stability and optimality," *Automatica*, vol. 36, no. 6, pp. 789–814, 2000.

[18] G. P. Incremona, A. Ferrara, and L. Magni, "Mpc for robot manipulators with integral sliding modes generation," *IEEE/ASME Transactions on Mechatronics*, vol. 22, no. 3, pp. 1299–1307, 2017.

[19] L. Dutta and D. Kumar Das, "Nonlinear disturbance observer based multiple-model adaptive explicit model predictive control for nonlinear mimo system," *International Journal of Robust and Nonlinear Control*, vol. 33, no. 11, pp. 5934–5955, 2023.

[20] D. Tavernini, M. Metzler, P. Gruber, and A. Sorniotti, "Explicit nonlinear model predictive control for electric vehicle traction control," *IEEE Transactions on Control Systems Technology*, vol. 27, no. 4, pp. 1438–1451, 2018.

[21] M. Santos, R. Galvao, and T. Yoneyama, "Robust model predictive control for a magnetic levitation system employing linear matrix inequalities," in *ABCM Symposium Series in Mechatronics*, vol. 4, 2010, pp. 147–155.

[22] Y. Qin, H. Peng, W. Ruan, J. Wu, and J. Gao, "A modeling and control approach to magnetic levitation system based on state-dependent arx model," *Journal of Process Control*, vol. 24, no. 1, pp. 93–112, 2014.

[23] M. Klaučo, M. Kaluz, and M. Kvasnica, "Real-time implementation of an explicit mpc-based reference governor for control of a magnetic levitation system," *Control Engineering Practice*, vol. 60, pp. 99–105, 2017.

[24] L. Dutta and D. K. Das, "A linear model predictive control design for magnetic levitation system," in *2020 International Conference on Computational Performance Evaluation (ComPE)*. IEEE, 2020, pp. 039–043.

[25] T. Bächle, S. Hentzelt, and K. Graichen, "Nonlinear model predictive control of a magnetic levitation system," *Control Engineering Practice*, vol. 21, no. 9, pp. 1250–1258, 2013.